Time reversal for inclusion detection in randomly layered media

D. G. Alfaro Vigo[1] **and K. Sølna**[2]

[1] Instituto de Matemática Pura e Aplicada–IMPA, Estrada D. Castorina 110, Rio de Janeiro, 22460-320, Brazil

[2] Dept. of Mathematics, University of California at Irvine, Irvine, CA 92697-3875, USA

E-mail: dgalfaro@impa.br, ksolna@math.uci.edu

Abstract. In this work we discuss detection of changes in a random medium when the measurements are not perfect, i.e. a noise from the electronic devices is included. We study a regime in which the typical length scales involved are well-separated. Moreover, since detection procedures based on the analysis of the reflected signals can fail because of the lack of coherency, we introduce a technique based on time reversal which can take advantage of *both* the coherent time-reversed signal and the additional incoherency induced by the measurement device.

We use asymptotic analysis of time-reversed signals in a changing medium to guide us in the selection of a statistical decision technique.

The proposed technique is illustrated by a series of numerical simulations. The results show a remarkable agreement with the asymptotic analysis and also highlight the robustness of this technique.

PACS numbers: 42.25.Dd, 43.60.Pt, 43.60.Bf

1. Introduction

Detection and imaging problems arise in various fields of science and technology (e.g. geophysics and medicine). In many situations the detection/imaging procedure relies on the propagation of a probing wave in the medium. In this context, special attention may have to be devoted to the situation when the propagation medium is heterogeneous on a fine scale.

Many of the conventional imaging methods use information provided by the direct reflection from the object of interest. In those cases a coherent reflected signal is produced by a large contrast in the impedance of the background medium, allowing one to establish the presence of an object and to estimate the distance from the object to the receiver. Other techniques admit a time reversal or cross correlation interpretation and consequently possess a statistical stabilization property which is important in a heterogeneous environment, see for instance [3, 1, 2]. Here, our focus will be on situations

when there is both strong medium heterogeneity as well as strong measurement noise so that the measured signal may not have a any discernible coherent component.

In [4], a detection/imaging procedure that uses physical time reversal was developed for the case where the macroscopic (effective) equation for the wave energy is a diffusion equation (this occurs for instance in the high-frequency regime when the random fluctuations of the medium are weak and isotropic). Their detection procedure allows for the presence of measurement errors in the time-reversed signal. A high contrast between the diffusion coefficients for the background and the inclusion allows the detection and characterization of the buried object.

More recently, in [5, 6] a detection/imaging procedure for a reflector embedded in a randomly layered medium based on physical time reversal was developed. The statistical stability of the time-reversed refocused signal allows the use of this procedure even when the reflected signal is not coherent (i.e. there is no contrast between the impedance of the background and the reflector). The presence of the reflector is detected from the information contained in the time reversal refocusing kernel. In fact, that information is extracted from a continuous family of time reversal refocusing kernels.

In this paper, we are interested in detecting an object buried in a randomly layered medium. We analyse a regime in which the probing pulse has a support larger than the random fluctuations of the medium and propagates deep into the medium. We use the measurements obtained after propagating the probing pulse in this medium, during two different periods of time in order to determine whether the properties of the medium has changed or not. When there is no coherent reflection and a relatively strong measurement noise is present the information contained in the measured reflected signals is not good enough to detect the inclusion. By time-reversing the difference of these reflected signals and back-propagating them into the medium we obtain a secondary reflection containing some coherent information. Unfortunately, if the noise level is relatively high, the signal to noise ratio is too low and it is difficult to detect the coherent signal. However, as we will show, the information contained in the random fluctuations induced by the measurements noise can still be very useful.

This paper is organized as follows, in Section 2 we briefly recall some key results about time reversal in a one-dimensional acoustic random medium. Section 3 is devoted to the presentation of time reversal in two media, and the generalization of related results obtained in previous works. In particular, we introduce here the time reversal of signal difference procedure that constitutes the basis of our detection technique. In Section 4, we introduce the detection technique by deriving the appropriate hypothesis test, after analysing the effect of measurements errors on the time-reversed signal difference and characterizing its asymptotic behaviour. The results obtained in numerical simulations are presented in Section 5 to show the reliability of the proposed detection technique.

2. Time reversal in a random medium

In this section we briefly present the asymptotic description of time reversal. We start by introducing the model equations for propagation of acoustic waves in a one-dimensional random medium. In this simplified framework, we are able to model and analyze the most important features of the wave propagation for the problem at hand. Subsequently, we shall use this analysis in a more complex setting.

2.1. One-dimensional acoustic model

We consider acoustic wave propagation in a one-dimensional heterogeneous medium modeled by the following equations for the pressure p and the velocity u

$$\varrho(z)\frac{\partial}{\partial t}u(z,t) + \frac{\partial}{\partial z}p(z,t) = 0 \tag{1a}$$

$$\frac{1}{K(z)}\frac{\partial}{\partial t}p(z,t) + \frac{\partial}{\partial z}u(z,t) = 0 \tag{1b}$$

where ϱ and K represent density and bulk modulus respectively.

We are interested in the situation where the medium consists of a homogeneous and a heterogeneous half-spaces separated by an interface. Furthermore, we assume that the medium properties in the heterogeneous half-space are rapidly varying and random. More specifically, the properties are characterized by a deterministic smoothly varying profile about which there are modulating random fluctuations.

We shall study the situation when an incident pulse can be used to probe the effective (background) medium. More specifically, we consider the asymptotic regime in which

$$\varepsilon \approx \frac{\text{fluctuations correl. length}}{\text{width of the pulse}} \approx \frac{\text{width of the pulse}}{\text{propagation distance}} \ll 1.$$

By considering an appropriate re-scaling of the space-time variables, and other involved magnitudes [7], we can rewrite the equations above in a dimensionless form. Accordingly, we assume that the medium properties are given by

$$\varrho(z) = \begin{cases} \varrho_0(z)(1+\eta^\varepsilon(z)), & \text{for } z \le 0 \\ \varrho_0(0), & \text{for } z > 0 \end{cases} \tag{2a}$$

$$K^{-1}(z) = \begin{cases} K_0^{-1}(z)(1+\mu^\varepsilon(z)), & \text{for } z \le 0 \\ K_0^{-1}(0), & \text{for } z > 0 \end{cases} \tag{2b}$$

where $\varrho_0(z)$ and $K_0(z)$ are the nonrandom (dimensionless) background density and bulk modulus, respectively, and $\eta^\varepsilon(z)$, $\mu^\varepsilon(z)$ are mean-zero, random functions. These are bounded (almost surely) by a deterministic constant $C > -1$ from below, and have correlation lengths of $\mathrm{O}(\varepsilon^2)$, where $\varepsilon \ll 1$, emphasizing that the disordered fluctuations are rapidly varying. This representation of the medium properties is consistent with the homogenization theory, the 'locally' homogenized medium properties are given by $\varrho_0(z)$

and $K_0(z)$. The corresponding homogenized (dimensionless) sound speed and acoustic impedance are given by

$$c_0(z) = \sqrt{\frac{K_0(z)}{\varrho_0(z)}} \quad \text{and} \quad \zeta_0(z) = \sqrt{\varrho_0(z)K_0(z)}, \tag{3}$$

respectively. For the fluctuations we use the following model

$$\eta^\varepsilon(z) = \eta(z, \frac{z}{\varepsilon^2}) \quad \text{and} \quad \mu^\varepsilon(z) = \mu(z, \frac{z}{\varepsilon^2}), \tag{4}$$

where for each fixed z, $\eta(z,s)$ and $\mu(z,s)$ are mean-zero, stationary stochastic processes with correlation lengths in s of O(1) (for example: the components of a stationary ergodic Markov process or a process with strong mixing properties). Since the fluctuations are not assumed to be small, this scaling is called *strong fluctuations regime*.

2.2. Time reversal in reflection

Next, we briefly obtain a representation of the refocused pulse for time reversal in reflection. We consider a regime/scaling in which the typical wavelength of the incident pulse is longer than the correlation length of the fluctuations, and where the wave propagates over a long distance. In this situation, the long term effect of the medium fluctuations plays an important role in the formation of a coherent refocused signal.

As the incident wave, we assume a downward traveling pulse that impinges upon the interface $z = 0$, it is described as a time signal given by

$$u_{\text{inc}}(0,t) = -\frac{\zeta_0^{-1/2}(0)f(\frac{t}{\varepsilon})}{2}, \qquad p_{\text{inc}}(0,t) = \frac{\zeta_0^{1/2}(0)f(\frac{t}{\varepsilon})}{2} \tag{5}$$

where f is a smooth function with compact support contained in $[0,+\infty)$. Here the time scaling emphasizes that the typical wavelength of the incident wave is of O(ε).

The corresponding signal scattered at the interface is given in terms of the reflection coefficient $R^\varepsilon(\omega)$ for the frequency ω as follows

$$u_{\text{ref}}(0,t) = \frac{\zeta_0^{-1/2}(0)B(t)}{2}, \qquad p_{\text{ref}}(0,t) = \frac{\zeta_0^{1/2}(0)B(t)}{2}, \tag{6}$$

with

$$B(t) = \frac{1}{2\pi}\int \mathrm{e}^{-\mathrm{i}\omega\frac{t}{\varepsilon}} R^\varepsilon(\omega)\hat{f}(\omega)\mathrm{d}\omega,$$

where $\hat{f}(\cdot)$ is the Fourier transform of the function $f(\cdot)$.

During the time reversal procedure, we record (part of) this reflected signal, at the Time Reversal Mirror (TRM), and re-emit it back into the random half-space after time-reversing its direction (i.e. the last recorded part is re-emitted first).

We characterize the TRM by the cutoff function $G_{t_0}(\cdot)$ supported on the recording time interval $[0,t_0]$ (or rapidly decaying outside it). Finally, we observe the time-reversed reflected signal in a scaled time window centred at t_1:

$$u_{\text{ref}}^{\text{TR}}(0,t_1+\varepsilon s) = \frac{\zeta_0^{-1/2}B_{t_0,t_1}^{\varepsilon,\text{TR}}(s)}{2}, \qquad p_{\text{ref}}^{\text{TR}}(0,t_1+\varepsilon s) = \frac{\zeta_0^{1/2}B_{t_0,t_1}^{\varepsilon,\text{TR}}(s)}{2},$$

where

$$B^{\varepsilon,\mathrm{TR}}_{t_0,t_1}(s) = \frac{1}{(2\pi)^2}\int\int \mathrm{e}^{\mathrm{i}\omega(\frac{t_1-t_0}{\varepsilon})}\mathrm{e}^{-\mathrm{i}\frac{h}{2}(t_1-t_0+\varepsilon s)}\mathrm{e}^{\mathrm{i}\omega s}\overline{\hat{f}}(\omega+\frac{\varepsilon}{2}h)\overline{\hat{G}_{t_0}}(h) \\ \times R^{\varepsilon}(\omega+\frac{\varepsilon}{2}h)\overline{R^{\varepsilon}}(\omega-\frac{\varepsilon}{2}h)\mathrm{d}\omega\mathrm{d}h.$$

Note that the recording and observation times t_0 and t_1, respectively, are O(1). Hence, the pulse travels a distance of O(1), which is much longer than its typical wavelength. Moreover, we observe the time-reversed reflected pulse in a time window scaled in accordance with the incident wave.

2.3. Time reversal asymptotics

Important information on the time-reversed acoustic field is obtained by an asymptotic analysis of $B^{\varepsilon,\mathrm{TR}}_{t_0,t_1}$ as ε approaches zero. This analysis relies on the characterization of the limiting statistical moments of the time-reversed reflection $B^{\varepsilon,\mathrm{TR}}_{t_0,t_1}(s)$ using a diffusion-approximation theorem.

In order to characterize the limiting statistical moments, we have to study the asymptotics of the correlations of the reflection coefficient at nearby frequencies. For instance, the asymptotics of $\mathbb{E}\{R^{\varepsilon}(\omega+\frac{\varepsilon}{2}h)\overline{R^{\varepsilon}}(\omega-\frac{\varepsilon}{2}h)\}$ is used to determine the limiting averaged time-reversed reflection.

The analysis yields

$$\lim_{\varepsilon\downarrow 0}\mathbb{E}\{R^{\varepsilon}(\omega+\frac{\varepsilon}{2}h)\overline{R^{\varepsilon}}(\omega-\frac{\varepsilon}{2}h)\} = \tilde{w}(\omega,h)$$

where $\tilde{w}(\omega,h) = \lim_{z\to-\infty} w(z,\psi;\omega,h)$, and $w(z,\psi;\omega,h)$ satisfies the Kolmogorov backward equation

$$(\frac{\partial}{\partial z}+\mathcal{L}^0_z)w = 0, \qquad \text{for } z<0 \tag{7}$$

with final condition $w|_{z=0} = \mathrm{e}^{\mathrm{i}\psi}$. The differential operator $\mathcal{L}^0_z$ is the generator of a diffusion on the circle, and is given by

$$\mathcal{L}^0_z = \frac{2h}{c_0(z)}\partial_\psi + 4\omega^2\frac{\alpha_n(z)}{c_0^2(z)}(1-\cos\psi)\partial^2_\psi$$

where

$$\alpha_n(z) = \int_0^\infty \mathbb{E}\{n(z,s)n(z,0)\}\mathrm{d}s, \qquad n(z,s) = \frac{\mu(z,s)-\eta(z,s)}{2}.$$

A further analysis leads to the following asymptotic description of the time-reversed reflection in probability:

$$\lim_{\varepsilon\downarrow 0} B^{\varepsilon,\mathrm{TR}}_{t_0,t_1}(s) = \begin{cases} B^{\mathrm{TR}}_{t_0}(s), & \text{when } t_0=t_1 \\ 0, & \text{otherwise,} \end{cases} \tag{8}$$

where

$$B^{\mathrm{TR}}_{t_0}(s) = \frac{1}{2\pi}\int \mathrm{e}^{\mathrm{i}\omega s}\widehat{K^{\mathrm{TR}}_{t_0}}(\omega)\overline{\hat{f}}(\omega)\,\mathrm{d}\omega = (K^{\mathrm{TR}}_{t_0}(\cdot)\star f(-\cdot))(s),$$

with $\star$, $\widehat{\cdot}$ denoting convolution with respect to t. The time reversal refocusing kernel $K_{t_0}^{\mathrm{TR}}(\cdot)$ is given through the following equations

$$\widehat{K_{t_0}^{\mathrm{TR}}}(\omega) = (\Lambda(\omega,\cdot) \star G_{t_0}(-\cdot))(0), \tag{9a}$$

$$\widehat{\Lambda(\omega,\cdot)}(h) = \tilde{w}(\omega,h). \tag{9b}$$

In the case where $G_{t_0}(\cdot) = \mathbf{1}_{[0,t_0]}(\cdot)$ (the indicator function of the interval $[0,t_0]$) (9a) simplifies to

$$\widehat{K_{t_0}^{\mathrm{TR}}}(\omega) = \int_0^{t_0} \Lambda(\omega,s)\,\mathrm{d}s. \tag{10}$$

In equation (8), we state that the refocusing takes place only when the recording and observation times coincide. Furthermore, the refocusing pulse is statistically stable, that is, it is deterministic.

The function $\Lambda(\omega,t)$ also appears in the characterization of the covariance function of the reflected signal [8], and it is called the *(normalized) power spectral density* of the reflected pulse.

2.4. Transport equations and the refocusing kernel

For a more detailed characterization of the refocusing kernel (9a), we proceed by solving equation (7) using a Fourier series in ψ

$$V(z,\psi;\omega,h) = \sum_{N=-\infty}^{\infty} V^N \mathrm{e}^{\mathrm{i}N\psi}.$$

We then obtain a system of backward stochastic differential equations for the coefficients V^N when $N \geq 0$

$$\frac{\partial V^N}{\partial z} + \frac{2\mathrm{i}hN}{c_0(z)} V^N + 2\omega^2 \frac{\alpha_n(z)}{c_0^2(z)} (\mathcal{T}V)^N = 0, \quad \text{for } z < 0$$

with the final conditions

$$V^N|_{z=0} = \delta_{N,1},$$

where the operator $(\mathcal{T}V)^N = (N+1)^2 V^{N+1} - 2N^2 V^N + (N-1)^2 V^{N-1}$ and $\delta_{M,S}$ represents the Kronecker delta. Furthermore, for $N < 0$ one gets that $V^N = 0$, and we finally have that

$$\tilde{w}(\omega,h) = \lim_{z\to-\infty} V^0(z;\omega,h).$$

Introducing the inverse Fourier transform

$$U^N = \frac{1}{2\pi} \int \mathrm{e}^{\mathrm{i}ht} V^N \mathrm{d}h, \qquad \text{for } N \geq 0, \tag{11}$$

and the travel time $\tau = \tau(z) = \int_z^0 c_0^{-1}(s)\mathrm{d}s$ as a new coordinate, we obtain the transport equations

$$\frac{\partial U^N}{\partial \tau} + 2N \frac{\partial U^N}{\partial t} - 2\omega^2 \beta_n(\tau) (\mathcal{T}U)^N = 0, \qquad \text{for } \tau > 0, \tag{12}$$

with the initial conditions

$$U^N|_{\tau=0} = \delta_{N,1}\delta(t), \tag{13}$$

where $\beta_n(\tau) = \alpha_n(\xi(\tau))/c_0(\xi(\tau))$, and $\xi(\tau)$ represents the inverse function of the travel time $\tau = \tau(z)$.

We obtained a system of hyperbolic partial differential equations, reflecting the fact that the waves propagate in the random medium with a finite speed. As a consequence, we have that

$$\Lambda(t,\omega) = U^0(\tau', t, \omega)$$

for any $\tau' \geq \frac{t}{2}$. Moreover, since we are interested in values of $t \leq t_0$, we have that

$$\Lambda(t,\omega) = U^0(\frac{t_0}{2}, t, \omega). \tag{14}$$

Therefore, if the cutoff function $G_{t_0}(\cdot) = \mathbf{1}_{[0,t_0]}(\cdot)$ then the refocusing kernel can be written as

$$\widehat{K_{t_0}^{\mathrm{TR}}}(\omega) = \int_0^{t_0} U^0(\frac{t_0}{2}, s, \omega)\,\mathrm{d}s. \tag{15}$$

3. Time reversal in two media

This section contains a generalization of some results that were presented in [9, 10], concerning time reversal in reflection in a changing medium. More specifically, in this paper we consider the case where the background as well as the random fluctuations of the media involved in the time reversal procedure are different. We allow the semi-infinite random medium to change, but assume that the homogeneous half-spaces remain unchanged. In the cited references, the background properties also remain unchanged.

The time reversal in reflection procedure in two media is now described as follows, a pulse traveling from the right impinges upon the interface $z = 0$, the reflected signal is recorded by a TRM during the time interval $[0, t_0]$, time reversed and sent back, now into a *different medium*. As a result after t_0 units of time, a coherent pulse traveling to the right emerges at the interface. This phenomenon is known as time reversal refocusing, and this emerging pulse is the so-called *refocused pulse*. In general, its shape is determined by the initial pulse waveform and the particular medium realization. Nevertheless, there are some interesting situations in which the form of the refocused pulse asymptotically does not depend on the media realizations but only on the medium statistics, i.e. it is *statistically stable* (or *self-averaging*).

Let the involved media be characterized by the densities $\varrho_j(z)$, and bulk moduli $K_j(z)$, where the index $j = 1, 2$ refers to the first or second medium, respectively. Furthermore, we have that

$$\varrho_j(z) = \begin{cases} \varrho_{j0}(z)(1 + \eta_j^\varepsilon(z)), & \text{for } z \leq 0 \\ \varrho_{j0}(0), & \text{for } z > 0 \end{cases} \tag{16a}$$

$$K_j^{-1}(z) = \begin{cases} K_{j0}^{-1}(z)(1 + \mu_j^\varepsilon(z)), & \text{for } z \leq 0 \\ K_{j0}^{-1}(0), & \text{for } z > 0 \end{cases} \tag{16b}$$

where $\varrho_{j0}(z)$ and $K_{j0}(z)$, represent the corresponding background properties, and $\eta_j^\varepsilon(z) = \eta_j(z, \frac{z}{\varepsilon^2})$, $\mu_j^\varepsilon(z) = \mu_j(z, \frac{z}{\varepsilon^2})$ their associated random fluctuations, $j = 1, 2$.

The effective (or background) sound speed and acoustic impedance are given by

$$c_{j0}(z) = \sqrt{\frac{K_{j0}(z)}{\varrho_{j0}(z)}} \quad \text{and} \quad \zeta_{j0}(z) = \sqrt{\varrho_{j0}(z)K_{j0}(z)},$$

respectively, with $j = 1, 2$.

The impinging acoustic pulse is the time signal given by (5). The scattering effect of the two random half-spaces is characterized by the reflection coefficients $R_j^\varepsilon(\omega)$, $j = 1, 2$. The cutoff function $G_{t_0}(\cdot)$ characterizes the TRM.

By observing the reflected signal at the interface, in a scaled time window centered at t_1, we have that

$$u_{\rm ref}^{\rm TR}(0, t_1 + \varepsilon s) = \frac{\zeta_0^{-1/2} B_{t_0,t_1}^{\varepsilon,{\rm TR}}(s)}{2}, \qquad p_{\rm ref}^{\rm TR}(0, t_1 + \varepsilon s) = \frac{\zeta_0^{1/2} B_{t_0,t_1}^{\varepsilon,{\rm TR}}(s)}{2},$$

with

$$B_{t_0,t_1}^{\varepsilon,{\rm TR}}(s) = \frac{1}{(2\pi)^2} \int\int {\rm e}^{{\rm i}\omega(\frac{t_1-t_0}{\varepsilon})} {\rm e}^{-{\rm i}\frac{h}{2}(t_1-t_0+\varepsilon s)} {\rm e}^{{\rm i}\omega s} \overline{\hat{f}}(\omega + \frac{\varepsilon}{2}h) \overline{\hat{G}_{t_0}}(h) \\ \times R_1^\varepsilon(\omega + \frac{\varepsilon}{2}h) \overline{R_2^\varepsilon}(\omega - \frac{\varepsilon}{2}h) {\rm d}\omega {\rm d}h.$$

Very useful information on the time-reversed acoustic field is obtained by analysing the asymptotic behaviour of the signal $B_{t_0,t_1}^{\varepsilon,{\rm TR}}(\cdot)$ as ε approaches zero. We briefly present this analysis in the next section.

3.1. Characterization of the limiting refocused pulse

The general characterization as $\varepsilon \downarrow 0$ of the refocused pulse is obtained by an asymptotic analysis of the time-reversed reflected signal $B_{t_0,t_1}^{\varepsilon,{\rm TR}}(s)$ using a diffusion-approximation theorem and the Itô formula. The calculations generalizes those presented in [9].

In the case where the recording and observation times are different, i.e. $t_1 \neq t_0$, it is very simple. Indeed, in this situation the fast phase ${\rm e}^{{\rm i}(\frac{t_1-t_0}{\varepsilon})}$ "kills" the integral and we have that $B_{t_0,t_1}^{\varepsilon,{\rm TR}}(s)$ converges in probability to the null process. This means that if we do not synchronize the recording and observation times, for $\varepsilon \ll 1$ we observe just a weak noisy signal.

For the case where $t_0 = t_1$, the description of the asymptotics of the process $B_{t_0}^{\varepsilon,{\rm TR}}(\cdot) = B_{t_0,t_0}^{\varepsilon,{\rm TR}}(\cdot)$ as $\varepsilon \downarrow 0$ is more complicated.

We introduce the differential operator

$$\mathcal{L}_z = h(\frac{1}{c_{10}(z)} + \frac{1}{c_{20}(z)})\partial_\psi + 4\omega^2 \Big\{ (\alpha_m(z) + \frac{1}{2}\alpha_n(z))(\frac{1}{c_{10}^2(z)} + \frac{1}{c_{20}^2(z)}) \\ - \frac{2}{c_{10}(z)c_{20}(z)} (\tilde{\alpha}_m(z) + \frac{1}{2}\tilde{\alpha}_n(z)\, \mathbf{1}_{\{\tau_1=\tau_2\}}(z) \cos\psi) \Big\} \partial_\psi^2 \qquad (17)$$

where

$$\alpha_m(z) = \int_0^\infty \mathbb{E}\{m_1(z,s)m_1(z,0)\}{\rm d}s = \int_0^\infty \mathbb{E}\{m_2(z,s)m_2(z,0)\}{\rm d}s$$

$$\tilde{\alpha}_m(z) = \int_0^\infty \mathbb{E}\{m_1(z,s)m_2(z,0)\}\mathrm{d}s = \int_0^\infty \mathbb{E}\{m_2(z,s)m_1(z,0)\}\mathrm{d}s$$
$$\alpha_n(z) = \int_0^\infty \mathbb{E}\{n_1(z,s)n_1(z,0)\}\mathrm{d}s = \int_0^\infty \mathbb{E}\{n_2(z,s)n_2(z,0)\}\mathrm{d}s$$
$$\tilde{\alpha}_n(z) = \int_0^\infty \mathbb{E}\{n_1(z,s)n_2(z,0)\}\mathrm{d}s = \int_0^\infty \mathbb{E}\{n_2(z,s)n_1(z,0)\}\mathrm{d}s$$

with

$$m_j(z,s) = \frac{1}{2}(\mu_j(z,s) + \eta_j(z,s))$$
$$n_j(z,s) = \frac{1}{2}(\mu_j(z,s) - \eta_j(z,s)), \quad j = 1,2.$$

Furthermore, $\mathbf{1}_{\{\tau_1=\tau_2\}}(\cdot)$ denotes the indicator function of the set $\{z \le 0 : \tau_1(z) = \tau_2(z)\}$ where $\tau_j(z) = \int_z^0 c_{j0}^{-1}(s)\mathrm{d}s$, $j = 1,2$ are the travel time from location z to the interface in the corresponding background medium.

Let W_s, be a standard one-dimensional Brownian motion with $s \in [0, +\infty)$ defined on a complete probability space. Define a new stochastic process $\tilde{W}_z$, $z \in (-\infty, 0]$ by setting $\tilde{W}_z = W_{-z}$ almost surely, this is a *backward (standard) one-dimensional Brownian motion*, which is a backward martingale [11]. The (backward) stochastic integral with respect to $\tilde{W}_z$ can be defined as

$$\int_{z_1}^{z_2} \xi(s) \overleftarrow{\mathrm{d}}\, \tilde{W}_s = -\int_{-z_2}^{-z_1} \xi(-s)\, \mathrm{d}W_s$$

where $\overleftarrow{\mathrm{d}}\, \tilde{W}_z$ represents the backward Itô's differential of $\tilde{W}_z$.

Consider the second order backward Itô stochastic partial differential equation

$$\mathrm{d}w + (\mathcal{L}_z w)\,\mathrm{d}z + 2\omega\sqrt{\gamma_m(z)}\,\partial_\psi w \overleftarrow{\mathrm{d}}\, \tilde{W}_z = 0, \qquad \text{for } z < 0 \tag{18}$$

with final condition

$$w|_{z=0} = \mathrm{e}^{\mathrm{i}\psi}, \tag{19}$$

where

$$\gamma_m(z) = 2\Big\{\alpha_m(z)\Big(\frac{1}{c_{10}^2(z)} + \frac{1}{c_{20}^2(z)}\Big) - 2\frac{\tilde{\alpha}_m(z)}{c_{10}(z)c_{20}(z)}\Big\}.$$

From [11, 12], we know that the stochastic equation (18) has a unique solution $w(z,\psi;\omega,h)$, which is a backward semimartingale.

Let us define

$$\tilde{w}(\omega,h) = \lim_{z\to-\infty} w(z,\psi;\omega,h) \tag{20}$$

and set

$$\widehat{\Lambda(\omega,\cdot)}(h) = \tilde{w}(\omega,h), \tag{21a}$$
$$\widehat{K_{t_0}^{\mathrm{TR}}}(\omega) = (\Lambda(\omega,\cdot) \star G_{t_0}(-\cdot))(0). \tag{21b}$$

Notice that in general these are random functions. In the important case where $G_{t_0}(\cdot) = \mathbf{1}_{[0,t_0]}(\cdot)$ (the indicator function of the interval $[0,t_0]$) (21b) simplifies to

$$\widehat{K_{t_0}^{\mathrm{TR}}}(\omega) = \int_0^{t_0} \Lambda(\omega,s)\,\mathrm{d}s. \tag{22}$$

Finally, we have that the time-reversed reflected signal $B_{t_0}^{\varepsilon,\mathrm{TR}}(s)$ converges in distribution as $\varepsilon \downarrow 0$ to the random signal

$$B_{t_0}^{\mathrm{TR}}(s) = (K_{t_0}^{\mathrm{TR}}(\cdot) \star f(-\cdot))(s) = \frac{1}{2\pi} \int \mathrm{e}^{\mathrm{i}\omega s} \widehat{K_{t_0}^{\mathrm{TR}}}(\omega) \overline{\hat{f}}(\omega)\, \mathrm{d}\omega \tag{23}$$

where the (random) time reversal refocusing kernel $K_{t_0}^{\mathrm{TR}}$ is given by (21*b*). In deriving this result, we first establish the tightness of this family of time-reversed signals to ensure that the limit exist. Then, using a diffusion-approximation theorem, we are able to characterize the limit of the corresponding finite-dimensional distributions by determining all their associated statistical moments. Finally, using the Itô formula one arrives to the representation above.

We next make some remarks about the stochastic equation (18). Note that it is not stochastic when $\gamma_m = 0$, a condition which is fulfilled if and only if $c_{10} = c_{20}$ and $\rho_m = \tilde{\alpha}_m/\alpha_m = 1$.

Let

$$Z_0 = \sup\{z \leq 0 : c_{10}(z) \neq c_{20}(z) \text{ or } \rho_m(z) \neq 1\},$$

with the understanding that if the set over which we take the supremum happens to be empty we put $Z_0 = -\infty$. In this particular case (i.e. when $Z_0 = -\infty$) we have that the refocused pulse is statistically stable, this is related to the fact that the propagation velocity remains unperturbed as was remarked in [10]. We refer to the interval $[Z_0, 0]$ as the *unperturbed propagation velocity region (or slab).*

Observe that the factor $\mathbf{1}_{\{\tau_1=\tau_2\}}(z)$ in (17) switches on and off the dependence of $\mathcal{L}_z$ on ψ, in particular if

$$Z_1 = \inf\{z \leq 0 : \tau_1(z) = \tau_2(z)\} > -\infty$$

one can explicitly find $w(z, \psi)$ for $z < Z_1$ as a function of $w_1(\psi) = w(Z_1^+, \psi)$. Furthermore, we obtain that

$$\tilde{w}(\omega, h) = \frac{1}{2\pi} \int_0^{2\pi} w_1(\psi; \omega, h)\, \mathrm{d}\psi. \tag{24}$$

In particular, if $Z_1 = 0$, we have that $\tilde{w}(\omega, h) = 0$ so the refocused pulse is the null signal. This is an extreme situation in which the travel time difference in the forward and backward propagation generates fast phases that ultimately annihilates the time-reversed reflected pulse. We called the interval $(-\infty, Z_1]$ *the asynchronous travel time region (or interval).*

3.1.1. Statistically stable refocusing It should be noted that statistical stability means that the limiting time reversed reflected signal (23) is deterministic and therefore the convergence occurs in probability. We now discuss an interesting situation in which we have a statistically stable refocusing.

Note that $-\infty \leq Z_1 \leq Z_0 \leq 0$. Suppose that $Z_0 = Z_1$, i.e. the unperturbed velocity and asynchronous travel time regions complement each other, then from the observations above we have that under this condition the refocusing is statistically stable. Indeed,

from the definition of Z_0 we get that $w(Z_0,\psi) = w(Z_1^+,\psi)$ is a deterministic function, thus from (24) and the representation given by (21*a*)-(21*b*) the result follows.

This is a very interesting situation in which the statistical stability comes from the fact that the propagation velocity remains unperturbed down to some depth below which the fast phase associated with the travel time difference kills out the effect of velocity perturbations.

This occurs for instance if $\delta c = c_{20} - c_{10} \geq 0$ (or ≤ 0), $\operatorname{supp}\delta c = [Z_1', Z_0']$ (or $\operatorname{supp}\delta c = (-\infty, Z_0']$) and $\rho_m(z) = 1$ for $Z_0' \leq z \leq 0$. In this case we say that the medium is changed by increasing (decreasing) the propagation velocity. We are specially interested in the case where δc is compactly supported as a model for the analysis of inclusion effects.

We remark that in the statistically stable case, for instance under the conditions stated before, we have convergence in probability whereas in the general situation the convergence occurs in distribution. This means that in the former case the refocused signal (for a small ε) remains close to the limiting deterministic signal (described by equations (18)–(21*b*) and (23)) with high probability.

Next, we continue to study the solution of (18) and its relationship with the refocusing kernel (21*b*).

3.2. Stochastic transport equations and the (random) refocusing kernel

We proceed by solving equation (18) using a Fourier series in ψ

$$V(z,\psi;\omega,h) = \sum_{N=-\infty}^{\infty} V^N \mathrm{e}^{\mathrm{i}N\psi}. \tag{25}$$

We obtain a system of backward stochastic differential equations for the coefficients V^N when $N \geq 0$

$$\mathrm{d}V^N + \Big\{\frac{2\mathrm{i}hN}{\bar{c}_0(z)}V^N + 2\omega^2[\beta_n(z)((N+1)^2V^{N+1} + (N-1)^2V^{N-1}) - \beta_{mn}(z)N^2V^N]\Big\}\mathrm{d}z$$
$$+2\mathrm{i}\omega\sqrt{\gamma_m(z)}NV^N \overleftarrow{\mathrm{d}}\,\tilde{W}_z = 0,$$

for $z < 0$ with the final conditions

$$V^N|_{z=0} = \delta_{N,1},$$

where $\delta_{M,S}$ represents the Kronecker delta and

$$\begin{aligned}
\frac{1}{\bar{c}_0(z)} &= \frac{1}{2}\Big(\frac{1}{c_{10}(z)} + \frac{1}{c_{20}(z)}\Big),\\
\beta_n(z) &= \frac{\tilde{\alpha}_n(z)}{c_{10}(z)c_{20}(z)}\mathbf{1}_{\{\tau_1=\tau_2\}}(z),\\
\beta_{mn}(z) &= \gamma_m(z) + \alpha_n(z)\Big(\frac{1}{c_{10}^2(z)} + \frac{1}{c_{20}^2(z)}\Big).
\end{aligned}$$

Furthermore, for $N < 0$ one gets that $V^N = 0$, and we finally have that

$$\tilde{w}(\omega,h) = \lim_{z\to-\infty} V^0(z;\omega,h).$$

Introducing the inverse Fourier transform

$$U^N(z,t,\omega) = \frac{1}{2\pi}\int \mathrm{e}^{\mathrm{i}ht} V^N(z;\omega,h)\mathrm{d}h, \qquad \text{for } N \geq 0, \tag{26}$$

and the averaged travel time $\bar{\tau} = (\tau_1(z) + \tau_2(z))/2$ as a new coordinate, we obtain the stochastic transport equations

$$\begin{aligned}\mathrm{d}U^N + 2N\frac{\partial U^N}{\partial t}\,\mathrm{d}\bar{\tau} = 2\omega^2\Big\{&\vartheta_n(\bar{\tau})[(N+1)^2U^{N+1} + (N-1)^2U^{N-1}] \\ &-\vartheta_{mn}(\bar{\tau})N^2U^N\Big\}\,\mathrm{d}\bar{\tau} + 2\mathrm{i}\omega\sqrt{\bar{\gamma}_m(\bar{\tau})}NU^N\,\mathrm{d}M_{\bar{\tau}}\end{aligned} \tag{27}$$

for $\bar{\tau} > 0$, $N \geq 0$, with $U^{-1} = 0$ and the initial conditions

$$U^N|_{\bar{\tau}=0} = \delta_{N,1}\delta(t). \tag{28}$$

The coefficients are given by

$$\begin{aligned}\bar{\gamma}_m(\bar{\tau}) &= \gamma_m(\xi(\bar{\tau})) \\ \vartheta_n(\bar{\tau}) &= \bar{c}_0(\xi(\bar{\tau}))\beta_n(\xi(\bar{\tau})) \\ \vartheta_{mn}(\bar{\tau}) &= \bar{c}_0(\xi(\bar{\tau}))\beta_{mn}(\xi(\bar{\tau}))\end{aligned}$$

where $\xi(\bar{\tau})$ represents the inverse function of the averaged travel time, $\mathrm{d}M_{\bar{\tau}}$ the Itô differential of the (forward) martingale $M_{\bar{\tau}} = W_{-\xi(\bar{\tau})}$ and $\delta(t)$ the Dirac δ-function.

This is a system of stochastic hyperbolic equations, reflecting the fact that the pulse propagates with a finite speed. As a consequence, we have that

$$\Lambda(t,\omega) = U^0(\bar{\tau}', t, \omega)$$

for any $\bar{\tau}' \geq \frac{t}{2}$. On the other hand, from (24) and (25) we have that $\tilde{w}(\omega,h) = V^0(Z_1^+;\omega,h)$, and consequently

$$\Lambda(t,\omega) = U^0(T_1, t, \omega) \tag{29}$$

where $T_1 = \tau_1(Z_1) = \tau_2(Z_1)$ is the time required to reach depth Z_1 and also the time required to get from there back to the interface. Therefore, if the cutoff function $G_{t_0}(\cdot) = \mathbf{1}_{[0,t_0]}(\cdot)$ then the refocusing kernel can be written as

$$\widehat{K_{t_0}^{\mathrm{TR}}}(\omega) = \int_0^{t_0} U^0(T_1 \wedge \frac{t_0}{2}, s, \omega)\,\mathrm{d}s \tag{30}$$

This means that the refocused pulse does not depend on the media properties below depth Z_1, regardless of how large the recording time t_0 is. In particular, when the unperturbed velocity and asynchronous travel time regions complement each other (i.e. $Z_0 = Z_1$) the refocused pulse does not carry information about the inclusion.

3.3. Time reversal of the signal difference

We introduce the time reversal of the signal difference corresponding to the two media. The reflections of similar pulses that impinges upon the interfaces of the initial and modified media are recorded. The difference of these reflected signals is time reversed and sent back into the modified medium by using a TRM. The corresponding secondary

reflections that emerge at the interface are called *time-reversed difference reflection*. The resulting signal correspond to the difference of two time-reversed signals, the first one obtained by time reversal in the modified medium (that remains unchanged during the procedure) and the second one corresponding to time reversal in a changing medium (i.e. involving these two media).

The time-reversed difference reflection $B^{\varepsilon,\mathrm{TRD}}_{t_0,t_1}(\cdot)$ can be characterized in a similar way as before. In fact, one gets the following asymptotics

$$\lim_{\varepsilon\downarrow 0} B^{\varepsilon,\mathrm{TRD}}_{t_0,t_1}(s) = \begin{cases} 0, & \text{(in probability) if } t_1 \neq t_0 \\ B^{\mathrm{TRD}}_{t_0}(s), & \text{(in distribution) if } t_1 = t_0 \end{cases} \tag{31}$$

The refocused limiting time-reversed difference reflection $B^{\mathrm{TRD}}_{t_0}$ is given as

$$B^{\mathrm{TRD}}_{t_0}(s) = (K^{\mathrm{TRD}}_{t_0}(\cdot) \star f(-\cdot))(s), \tag{32}$$

where

$$\widehat{K^{\mathrm{TRD}}_{t_0}}(\omega) = (\Lambda^{\mathrm{D}}_{12}(\omega,\cdot) \star G_{t_0}(-\cdot))(0), \tag{33a}$$

$$\widehat{\Lambda^{\mathrm{D}}_{12}(\omega,\cdot)}(h) = \tilde{w}_{22}(\omega,h) - \tilde{w}_{12}(\omega,h). \tag{33b}$$

Furthermore, $\tilde{w}_{22}(\omega,h) = \lim_{z\to-\infty} w(z,\psi;\omega,h)$ where $w(z,\psi)$ solves the Kolmogorov backward equation

$$(\partial_z + \mathcal{L}^0_z)w = 0, \qquad \text{for } z < 0 \tag{34}$$

with the final condition $w|_{z=0} = \mathrm{e}^{\mathrm{i}\psi}$, where the generator is given by

$$\mathcal{L}^0_z = \frac{2h}{c_{20}(z)}\partial_\psi + 4\omega^2 \frac{\alpha_n(z)}{c^2_{20}(z)}(1-\cos\psi)\,\partial^2_\psi.$$

On the other hand $\tilde{w}_{12}(\omega,h) = \lim_{z\to-\infty} w(z,\psi;\omega,h)$ where $w(z,\psi)$ solves the stochastic partial differential equation (18).

Notice that $\tilde{w}_{22}$ corresponds to time reversal in the modified medium while it remains unchanged during the time reversal procedure, whereas $\tilde{w}_{12}$ comes from time reversal in a changing medium (propagating forward in the initial medium and backward in the modified one). Consequently, if the refocused pulse for time reversal in a changing medium is statistically stable then the time-reversed difference reflection also has this property.

We have the following representation for the time reversal difference refocusing kernel

$$\widehat{K^{\mathrm{TRD}}_{t_0}}(\omega) = \int G_{t_0}(s)(U^0_{22}(\frac{t_0}{2},s,\omega) - U^0_{12}(T_1 \wedge \frac{t_0}{2},s,\omega))\,\mathrm{d}s$$

where U^N_{22}, $N \geq 0$ satisfy the transport equations

$$\frac{\partial U^N}{\partial \tau} + 2N\frac{\partial U^N}{\partial t} = 2\omega^2 \frac{\alpha_n(\xi_2(\tau))}{c_{20}(\xi_2(\tau))}(\mathcal{T}U)^N \tag{35}$$

with initial conditions (28). The operator

$$(\mathcal{T}U)^N = (N+1)^2 U^{N+1} - 2N^2 U^N + (N-1)^2 U^{N-1}$$

and $\xi_2(\tau)$ represents the inverse of the function $\tau(z) = \int_z^0 c_{20}^{-1}(s)\mathrm{d}s$. Furthermore, U_{12}^N, $N \geq 0$ solve the stochastic transport equations (27) with similar initial conditions.

Moreover, if the cutoff function $G_{t_0}(\cdot) = \mathbf{1}_{[0,t_0]}(\cdot)$, then

$$\widehat{K_{t_0}^{\mathrm{TRD}}}(\omega) = \int_0^{t_0} (U_{22}^0(\frac{t_0}{2}, s, \omega) - U_{12}^0(T_1 \wedge \frac{t_0}{2}, s, \omega))\,\mathrm{d}s$$

which in the case where the unperturbed velocity and asynchronous travel time regions complement each other (i.e. $Z_0 = Z_1$), can be re-written as

$$\widehat{K_{t_0}^{\mathrm{TRD}}}(\omega) = \int_0^{t_0} (U_{22}^0(\frac{t_0}{2}, s, \omega) - U_{22}^0(T_0 \wedge \frac{t_0}{2}, s, \omega))\,\mathrm{d}s. \tag{36}$$

Notice, that when the incident pulse does not penetrate into the medium modifications (i.e. $t_0/2 < T_0$) the time-reversed difference reflection is the null signal.

4. Time reversal detection

4.1. Detection problem

We now return to the problem of detecting changes in a highly heterogeneous medium. We probe the medium during different periods of time and want to know if any change has occurred in the medium properties. More specifically, if we think of the medium during these two periods of time, as been modeled by equations (16*a*) (for media '1' and '2'), we are interesting in determining if $c_{20}(z) \neq c_{10}(z)$. To probe the media we use an incident pulse that scales as (5), and search for information in the reflected signal but when there is no coherent reflection, all the information is hidden in the noisy signals and a straightforward application of detection techniques are difficult to use, because of the low signal to noise ratio. Nevertheless, the statistics of the reflected signals are well understood and it is possible to extract information about the medium properties (see [13, 14, 8]).

We introduce here a method based on the time reversal difference procedure presented in section 3.3 and a hypothesis testing technique, that is advantageous relative to just using the reflected signals. Since the time reversal difference procedure yields a coherent signal, one usually has a high signal to noise ratio and therefore standard detection techniques perform well. Moreover, when the refocused signal is statistically stable the randomness associated with the medium fluctuations is reduced to a minimum level and consequently good performance of the detection technique. We shall show that our approach works well in very noisy environments. First, we present important aspects concerning the modeling and begin by introducing the measurement errors.

4.2. Measured time-reversed difference reflection

As a result of the data acquisition process, some errors are introduced in the measured quantities. The quantities we are interesting in are signals smoothly varying on the scale ε. Consequently, the error introduced during a direct measurement is modeled as

an additive 'noise' with the corresponding scaling, that is the measured signal $g^{\varepsilon}_{\text{meas}}(t)$ associated with the actual signal $g^{\varepsilon}(t)$ is given as

$$g^{\varepsilon}_{\text{meas}}(t) = g^{\varepsilon}(t) + \nu(\frac{t}{\varepsilon})$$

where $\nu(\cdot)$ is a mean zero, stationary Gaussian random process defined on a certain probability space $(\mathrm{N}, \mathcal{N}, P)$. Note that the noise is fluctuating on the same scale as the incoherent wave reflections. We have the following representations for noise process and its covariance

$$\nu(s) = \int \mathrm{e}^{\mathrm{i}\omega s}\Phi_{\nu}(\mathrm{d}\omega), \qquad E\{\nu(s)\nu(0)\} = \int \mathrm{e}^{\mathrm{i}\omega s}F_{\nu}(\mathrm{d}\omega)$$

where $\Phi_{\nu}(\cdot)$ and $F_{\nu}(\cdot)$ are the so called *random spectral* and *power spectral measures*, respectively [15] and $E\{\cdot\}$ represents expectation with respect to the probability measure P. Furthermore, the measurement error intensity is characterized by

$$\sigma^2_{\nu} = E\{\nu^2(0)\} = \int F_{\nu}(\mathrm{d}\omega).$$

During the time reversal procedure we introduce direct measurement errors three times, during the acquisition of the two primary reflected signals and also the refocused signal. We assume that these direct noise sources are statistically independent. Consequently, the measurement error in the whole time reversal procedure is given by the random vector-process $\boldsymbol{\nu} = (\nu_1, \nu_2, \nu_3)$ defined on the product space $\mathbf{N} = \mathrm{N}\times\mathrm{N}\times\mathrm{N}$ with the corresponding product measure, and $\boldsymbol{\nu}(\cdot, \mathbf{n}) = (\nu_1(\cdot, n_1), \nu_2(\cdot, n_2), \nu_3(\cdot, n_3))$ where $\mathbf{n} = (n_1, n_2, n_3) \in \mathbf{N}$.

After some straightforward calculations we get that

$$B^{\varepsilon,\text{TRD}}_{t_0,\text{meas}}(s) = B^{\varepsilon,\text{TRD}}_{t_0}(s) + B^{\varepsilon}_{t_0,\boldsymbol{\nu}}(s) \tag{37a}$$

$$B^{\varepsilon}_{t_0,\boldsymbol{\nu}}(s) = B^{\varepsilon}_{t_0,\delta\nu}(s) + \nu_3(s). \tag{37b}$$

The first term in the decomposition of (37a) represents the actual time reversal signal difference (when no errors are introduced during the process) and the second is associated with measurements errors. Moreover, it arises from the propagation of the difference of the direct measurements noise associated with the primary reflections $\delta\nu(\cdot) = \nu_2(\cdot) - \nu_1(\cdot)$ and the error in the direct measurement of the time-reversed difference reflection (cf. (37b)). The primary reflections propagated noise can be written as

$$B^{\varepsilon}_{t_0,\delta\nu}(s) = \frac{1}{2\pi}\int\int \mathrm{e}^{\mathrm{i}(\omega-\varepsilon h)s}R^{\varepsilon}_2(\omega-\varepsilon h)\hat{G}_{t_0}(h)\Phi_{\delta\nu}(\mathrm{d}\omega)\mathrm{d}h$$

where $\Phi_{\delta\nu}(\cdot)$ is the random spectral measure on $\mathbf{N}$ given by

$$\Phi_{\delta\nu}(\cdot, \mathbf{n}) = \Phi_{\nu}(\cdot, n_2) - \Phi_{\nu}(\cdot, n_1)$$

for $\mathbf{n} = (n_1, n_2, n_3) \in \mathbf{N}$.

4.3. Asymptotics of the measured time-reversed difference reflection

We now focus our analysis on the case where the velocity changes in an increasing/decreasing fashion. This implies that $B_{t_0}^{\varepsilon,\mathrm{TRD}}(s)$ converges in probability to the deterministic signal $B_{t_0}^{\mathrm{TRD}}(s)$ given by (32).

By using that the random process $\delta\nu(\cdot)$ is stationary, Gaussian and centred and the asymptotics for the moments of the reflection coefficient R_2^ε one can establish the convergence in distribution as $\varepsilon \downarrow 0$ of $B_{t_0,\delta\nu}^\varepsilon(s)$ to a stationary, centred Gaussian process $B_{t_0,\delta\nu}(s)$ with covariance function given by

$$C_{t_0,\delta\nu}(s) = 2\int \mathrm{e}^{\mathrm{i}\omega s}\widehat{K_{t_0,2}^{\mathrm{R}}}(\omega)F_\nu(\mathrm{d}\omega) \tag{38}$$

where

$$\widehat{K_{t_0,2}^{\mathrm{R}}}(\omega) = (\Lambda_{22}(\omega,\cdot)\star G_{t_0}^2(-\cdot))(0) = \int \Lambda_{22}(\omega,s)G_{t_0}^2(s)\mathrm{d}s, \tag{39a}$$

$$\widehat{\Lambda_{22}(\omega,\cdot)}(h) = \tilde{w}_{22}(\omega,h) = \lim_{z\to-\infty} w(z,\psi;\omega,h), \tag{39b}$$

and $w(z,\psi)$ satisfies the partial differential equation (34).

Furthermore, since $\delta\nu(\cdot)$ and $\nu_3(\cdot)$ are statistically independent we finally get that $B_{t_0,\boldsymbol{\nu}}^\varepsilon(s)$ converges in distribution as $\varepsilon \downarrow 0$ to a mean zero, stationary, Gaussian random process with a covariance function given by

$$C_{t_0,\boldsymbol{\nu}}(s) = \int \mathrm{e}^{\mathrm{i}\omega s}(1+2\widehat{K_{t_0,2}^{\mathrm{R}}}(\omega))F_\nu(\mathrm{d}\omega). \tag{40}$$

Finally, from the Slutsky's theorem [16], it follows that $B_{t_0,\mathrm{meas}}^{\varepsilon,\mathrm{TRD}}(s)$ converges in distribution as $\varepsilon \downarrow 0$ to a Gaussian random process with mean $B_{t_0}^{\mathrm{TRD}}(s)$ given by (32) and covariance function given by (40).

We remark that for time reversal in a random medium which remains fixed, a similar analysis of the measured refocused pulse yields the convergence in distribution to a Gaussian random process whose mean is the limiting deterministic refocused signal and the covariance function is similar to (40) except for the prefactor 2. Moreover, for time reversal in a changing medium a similar result holds as long as the limiting refocused signal (when no error measurements are present) is deterministic.

4.4. Statistical test

The detection problem can be stated as a hypothesis testing problem for the following general hypotheses:

H_0: there are no changes in the medium (null hypothesis)

H_a: the medium has changed (alternate hypothesis)

According to the general theory of hypothesis testing [17], the statistical test consists of a procedure to decide whether the null hypothesis can be accepted or rejected. In general, a region in the space where the sample lives is selected and when the sample belongs to it the hypothesis is rejected. This region is the so-called *rejection region*. In a

test two types of independent errors can be made. Type I errors correspond to rejecting H_0 when it is correct (false alarm) and type II errors to accepting H_0 when it is false (missed detection). Their probabilities play an important role in the design of a test.

The probability of type I errors is given by

$$\alpha = \Pr\{\text{rejecting } \mathrm{H}_0 \,|\, \mathrm{H}_0 \text{ is true}\},$$

while the probability of type II errors is expressed as

$$\beta = \Pr\{\text{accepting } \mathrm{H}_0 \,|\, \mathrm{H}_\mathrm{a} \text{ is true}\}.$$

Since generally, both errors can not be kept small at the same time a guideline for designing the test is to select the rejection region in such a way that the probability of type II errors (β) is minimized when the probability of type I errors (α) is fixed. The probability α is called the *level of significance of the test*. The success of the test (probability of detection) is called the *power of the test* and equals $1-\beta$. In detection applications it is usually presented graphically as the Receiver Operating Curve (ROC) that represents the power of the test as a function of the level of significance.

The asymptotic description of the measured time reversal difference signal as a Gaussian random process presented above allows us to select an appropriate statistical test for this detection problem. In what follows, we consider the detection problem for the asymptotic characterization of the measured time reversal difference signal.

We consider the (finite) discrete time sampling of the time reversed signal $\mathbf{x} = (B^{\mathrm{TRD}}_{t_0,\mathrm{meas}}(s_1), \cdots, B^{\mathrm{TRD}}_{t_0,\mathrm{meas}}(s_M))^t$ with uniform sampling rate $h = s_{j+1} - s_j$ and centred at 0 ($= (s_1 + s_M)/2$). The hypotheses can be reformulated as follows

H_0: $\mathbf{x}$ is a sample of the random variable $\mathbf{X}_0 \sim \mathcal{N}(\mathbf{0}, \mathbf{C}_0)$

H_a: $\mathbf{x}$ is a sample of a random variable $\mathbf{X}_a \sim \mathcal{N}(\boldsymbol{\mu}_\mathrm{a}, \mathbf{C}_\mathrm{a})$,

where the mean vector $\boldsymbol{\mu}_\mathrm{a} = (B^{\mathrm{TRD}}_{t_0}(s_1), \cdots, B^{\mathrm{TRD}}_{t_0}(s_M))^t$ with the $B^{\mathrm{TRD}}_{t_0}(\cdot)$ given by (32) and the elements of the covariance matrices $(\mathbf{C}_0)_{ij}$, $(\mathbf{C}_\mathrm{a})_{ij}$ are of the form $C_{t_0,\boldsymbol{\nu}}((j-i)h)$ given by (38) with $K^{\mathrm{R}}_{t_0,2}(\cdot)$ corresponding to the initial and second (changed) media, respectively.

The covariance matrices are symmetric Toeplitz matrices. Furthermore, if the power spectral measure of the measurement noise is absolutely continuous with a Radon-Nikodym derivative $f_\nu(\omega) = F_\nu(\mathrm{d}\omega)/\mathrm{d}\omega$ in $L^1(\mathbb{R})$ then we have that

$$(\mathbf{C}_0)_{ij} = \frac{1}{2\pi}\int_{-\pi}^{\pi} \mathrm{e}^{\mathrm{i}(j-i)\lambda}\tilde{f}_0(\lambda)\mathrm{d}\lambda$$

$$(\mathbf{C}_\mathrm{a})_{ij} = \frac{1}{2\pi}\int_{-\pi}^{\pi} \mathrm{e}^{\mathrm{i}(j-i)\lambda}\tilde{f}_\mathrm{a}(\lambda)\mathrm{d}\lambda$$

where

$$\tilde{f}_\cdot(\lambda) = \frac{2\pi}{h}\sum_{k=-\infty}^{\infty} f_\nu\Big(\frac{\lambda+2k\pi}{h}\Big)\Big(1 + 2\widehat{K^{\mathrm{R}}_{t_0,2}}\Big(\frac{\lambda+2k\pi}{h}\Big)\Big) \tag{41}$$

with $K^{\mathrm{R}}_{t_0,2}(\cdot)$ corresponding to the initial and second (changed) media in the expressions for $\tilde{f}_0$ and $\tilde{f}_\mathrm{a}$, respectively. In order to explicitly write the dependence of the covariance matrix on the function $\tilde{f}_\cdot(\cdot)$, we set $\mathbf{C}_0 = T_M(\tilde{f}_0)$ and $\mathbf{C}_\mathrm{a} = T_M(\tilde{f}_\mathrm{a})$.

Let us introduce the function

$$\tilde{f}(\lambda) = \frac{2\pi}{h} \sum_{k=-\infty}^{\infty} f_\nu(\frac{\lambda + 2k\pi}{h}),$$

and its extreme values $m_{\tilde{f}} = \operatorname{ess\,inf} \tilde{f}$, $M_{\tilde{f}} = \operatorname{ess\,sup} \tilde{f}$. Since $f_\nu(\lambda) \geq 0$ and $0 \leq \widehat{K^{\mathrm{R}}_{t_0,2}}(\lambda) \leq 1$, we get that

$$\operatorname{ess\,inf} \tilde{f}_{\mathrm{a}} = m_{\tilde{f}_{\mathrm{a}}} \geq m_{\tilde{f}}, \qquad \operatorname{ess\,sup} \tilde{f}_{\mathrm{a}} = M_{\tilde{f}_{\mathrm{a}}} \leq 3M_{\tilde{f}}. \tag{42}$$

Consequently, the corresponding Toeplitz determinant $|T_M(\tilde{f}_{\mathrm{a}})|$ satisfies the estimates

$$(m_{\tilde{f}})^M \leq |T_M(\tilde{f}_{\mathrm{a}})| \leq (3M_{\tilde{f}})^M.$$

In what follows, we assume that $m_{\tilde{f}} > 0$.

In general, the covariance matrix $\mathbf{C}_0$ is unknown, however it can be estimated by performing a time reversal experiment in the unchanged medium. (In the case of a homogeneous medium it can be explicitly computed from equation (38).) Thus, we now assume that $\mathbf{C}_0$ is given, or equivalently that we know $\tilde{f}_0$. Concerning the covariance matrix $\mathbf{C}_{\mathrm{a}}$, since it is completely characterized by $\tilde{f}_{\mathrm{a}}$, we assume that a set of admissible functions $\tilde{\mathcal{F}}$ is given.

We can reformulate the problem as follows: *given a sample* $\mathbf{x}$ *of a random variable distributed as* $\mathcal{N}(\boldsymbol{\mu}, \mathbf{C})$ *test the hypotheses* H_0 *vs.* H_{a}, where

- H_0: $\boldsymbol{\mu} = \mathbf{0}$ and $\mathbf{C} = \mathbf{C}_0$
- H_{a}: $\boldsymbol{\mu} \neq \mathbf{0}$ and $\mathbf{C} = T_M(\tilde{f})$ with $\tilde{f} \in \tilde{\mathcal{F}}$.

The set $\tilde{\mathcal{F}}$ consists of the functions that can be represented as in (41), where the kernel $K^{\mathrm{R}}_{t_0,2}$ corresponds to an admissible random medium through the relations (39*a*)-(39*b*). Here we consider the set of functions $\tilde{f}_{\mathrm{a}}$ satisfying (42).

4.4.1. The Maximum Likelihood Ratio Test The Neyman-Pearson lemma indicates an effective way for selecting the rejection region [17], that leads to the *Maximum Likelihood Ratio (MLR) Test*. Although in the situation at hand this criterion does not give an optimal result, we consider it as a starting point. Later on, after some asymptotic analysis we shall slightly modify this test in order to achieve a better performance.

The *rejection region* at significance level α is given by $R_\alpha = \{\mathbf{x} : \Gamma(\mathbf{x}) \geq c_\alpha\}$ where

$$\Gamma(\mathbf{x}) = \frac{\sup_{\boldsymbol{\mu}\neq\mathbf{0}, f\in\tilde{\mathcal{F}}} |T_M(f)|^{-1/2} \exp\{-\frac{1}{2}(\mathbf{x}-\boldsymbol{\mu})^t T_M^{-1}(f)(\mathbf{x}-\boldsymbol{\mu})\}}{|\mathbf{C}_0|^{-1/2} \exp\{-\frac{1}{2}\mathbf{x}^t \mathbf{C}_0^{-1}\mathbf{x}\}},$$

and c_α is determined from the equation $\Pr\{\mathbf{x} \in R_\alpha |\, H_0\} = \alpha$.

After some simple algebra, we arrive at the *test statistic* $Q_M(\mathbf{x}) = \mathbf{x}^t \mathbf{C}_0^{-1} \mathbf{x}$ and get that $R_\alpha = \{\mathbf{x} : Q_M(\mathbf{x}) \geq \chi^2_M(1-\alpha)\}$, where $\chi^2_M(\cdot)$ represents the inverse of the cumulative χ^2-distribution function with M degrees of freedom. This is a consequence of the boundedness of $|T_M(f)|$ and the fact that under H_0, $Q_M(\mathbf{x})$ has a χ^2-distribution with M degrees of freedom.

In order to measure the performance of the test, we now have to determine its power as a function of the significance level, i.e. the probability of rejection under the alternate hypothesis for each value of α. Since the alternate hypothesis is composite the power of the test is parameterized by the mean vector $\boldsymbol{\mu}$ and the covariance matrix $\mathbf{C}$. We find $P(\alpha;\boldsymbol{\mu},\mathbf{C}) = \Pr\{\mathbf{x}^t\mathbf{C}_0^{-1}\mathbf{x} \geq \chi^2_M(1-\alpha)|\,\mathbf{x}\sim\mathcal{N}(\boldsymbol{\mu},\mathbf{C})\}$. This is the complement of the cumulative distribution function for a quadratic form of a normally distributed random variable, and we have [18] that $P(\alpha;\boldsymbol{\mu},\mathbf{C}) = G(\chi^2_M(1-\alpha);\boldsymbol{\lambda},\boldsymbol{\xi})$. The function $G(\cdot)$ corresponds to the complement of the cumulative distribution function of the random variable $\sum_{j=1}^M \lambda_j(W_j-\xi_j)^2$ where the W_j's are mutually independent $\mathcal{N}(0,1)$ random variables, the λ_j's are the eigenvalues of the matrix $\mathbf{C}\mathbf{C}_0^{-1}$, the vector $\boldsymbol{\xi} = \mathbf{O}^t\mathbf{L}^{-1}\boldsymbol{\mu}$, $\mathbf{L}$ is the lower triangular matrix in the Cholesky decomposition of $\mathbf{C}$ and $\mathbf{O}$ is an orthogonal matrix formed by the eigenvectors of $\mathbf{L}^t\mathbf{C}_0^{-1}\mathbf{L}$. Furthermore, we have the following integral representation

$$G(q;\boldsymbol{\lambda},\boldsymbol{\xi}) = \int_{-\mathrm{i}\infty}^{+\mathrm{i}\infty} \frac{\exp(-qu+\phi(u))}{u}\,\mathrm{d}u, \tag{43}$$

where the path of integration is indented toward the right at $u=0$, and we have set

$$\phi(u) = \frac{1}{2}\sum_{j=1}^M \{\xi_j^2(\frac{1}{1-2u\lambda_j}-1) - \log(1-2u\lambda_j)\}.$$

This integral can be efficiently evaluated with a high accuracy by using a Gauss-Chebyshev quadrature formula [19].

4.4.2. Asymptotics of the MLR test statistic In this section we study the asymptotic behaviour for large M of the scaled test statistic $\tilde{Q}_M(\mathbf{x}) = Q_M(\mathbf{x})/M$ when $\mathbf{x}\sim\mathcal{N}(\boldsymbol{\mu},\mathbf{C})$.

The mean and variance of $\tilde{Q}_M$ are given by

$$\tilde{\mu}_{Q,M} = \frac{1}{M}\{\mathrm{Tr}(\mathbf{C}\mathbf{C}_0^{-1}) + \boldsymbol{\mu}^t\mathbf{C}_0^{-1}\boldsymbol{\mu}\} = \frac{1}{M}\sum_{j=1}^M \lambda_j(1+\xi_j^2),$$

$$\tilde{\sigma}^2_{Q,M} = \frac{2}{M^2}\{\mathrm{Tr}(\mathbf{C}\mathbf{C}_0^{-1})^2 + 2\boldsymbol{\mu}^t\mathbf{C}_0^{-1}\mathbf{C}\mathbf{C}_0^{-1}\boldsymbol{\mu}\} = \frac{2}{M^2}\sum_{j=1}^M \lambda_j^2(1+2\xi_j^2).$$

Consider the normalized statistics $z_M = (\tilde{Q}_M - \tilde{\mu}_{Q,M})/\tilde{\sigma}_{Q,M}$. We claim that *the random variable z_M is asymptotically normally distributed as $\mathcal{N}(0,1)$ for large M.*

The characteristic function $\psi_M(u) = \mathbb{E}\{\mathrm{e}^{\mathrm{i}uz_M}\}$ is given by

$$\log\psi_M(u) = \frac{1}{2}\sum_{j=1}^M \{\xi_j^2(\frac{1}{1-2\mathrm{i}\tilde{u}\tilde{\lambda}_j}-1) - \log(1-2\mathrm{i}\tilde{u}\tilde{\lambda}_j)\} - \mathrm{i}\tilde{u}\tilde{\mu}_{Q,M}$$

where $\tilde{u} = \frac{u}{\tilde{\sigma}_{Q,M}}$ and $\tilde{\lambda}_j = M^{-1}\lambda_j$. Furthermore, we have the following estimate

$$\log\psi_M(u) = \frac{u^2}{2} + r_M,$$

$$|r_M| \leq A|\frac{u}{\tilde{\sigma}_{Q,M}}|^3 \sum_{j=1}^{M}(1+\xi_j^2)\tilde{\lambda}_j^3.$$

where the constant A does not depend on M. Consequently, it is enough to prove that $r_M \to 0$ as $M \to +\infty$.

Since, the covariance matrices are Toeplitz matrices, we get the following (uniformly in M) bounds for the eigenvalues of $\mathbf{C}\mathbf{C}_0^{-1}$ [20]

$$0 < \frac{m_{\tilde{f}}}{3M_{\tilde{f}}} \leq \operatorname{ess\,inf}(\tilde{f}_{\mathrm{a}}/\tilde{f}_0) \leq \lambda_j \leq \operatorname{ess\,sup}(\tilde{f}_{\mathrm{a}}/\tilde{f}_0) \leq \frac{3M_{\tilde{f}}}{m_{\tilde{f}}} < +\infty. \tag{44}$$

As a consequence, one has the estimates

$$\tilde{\sigma}_{Q,M}^2 \geq \frac{2}{M^2}\sum_{j=1}^{M}\lambda_j^2 \geq \frac{A_1}{M}.$$

Moreover, one can obtain uniform bounds similar to (44), for the eigenvalues of the covariance matrices $\mathbf{C}_0$ and $\mathbf{C}$. Consequently, we get the estimates

$$\begin{aligned}\sum_{j=1}^{M}(1+\xi_j^2)\tilde{\lambda}_j^3 &\leq \frac{A_2}{M^2} + \frac{|\boldsymbol{\mu}^t\mathbf{C}_0^{-1}(\mathbf{C}\mathbf{C}_0^{-1})^2\boldsymbol{\mu}|}{M^3} \leq \frac{A_2}{M^2} + \frac{\|\mathbf{C}_0^{-1}\boldsymbol{\mu}\|\|(\mathbf{C}\mathbf{C}_0^{-1})^2\boldsymbol{\mu}\|}{M^3}\\ &\leq \frac{A_2}{M^2} + \frac{A_3\|\boldsymbol{\mu}\|^2}{M^3} \leq \frac{A_2 + A_3\|\boldsymbol{\mu}\|_\infty^2}{M^2} \leq \frac{A_2'}{M^2}.\end{aligned}$$

Thus, we have that $|r_M| \leq A'|u|^3M^{-1/2}$ and the claim follows.

Next, we focus on the asymptotic behaviour of the power of the test. Let us assume that $\sum_{j=1}^{M}\mu_j^2 < \infty$ uniformly in M and the set of admissible functions $\mathcal{F}_{\mathrm{a}}$ is contained within the Wiener class (in other words the series $\sum_{j=0}^{\infty}C_{t_0,\boldsymbol{\nu}}(jh)$ are absolutely convergent). Applying Szegö's theorem on the distribution of eigenvalues of Toeplitz matrices [20], one gets that

$$\begin{aligned}\tilde{\mu}_{Q,M} &= \frac{1}{2\pi}\int_{-\pi}^{\pi}\frac{\tilde{f}_{\mathrm{a}}(s)}{\tilde{f}_0(s)}\,\mathrm{d}s + \mathrm{o}(1) = \langle\tilde{f}_{\mathrm{a}}/\tilde{f}_0\rangle + \mathrm{o}(1),\\ \tilde{\sigma}_{Q,M}^2 &= \frac{1}{M\pi}\int_{-\pi}^{\pi}\Big[\frac{\tilde{f}_{\mathrm{a}}(s)}{\tilde{f}_0(s)}\Big]^2\mathrm{d}s + \mathrm{o}(\frac{1}{M}) = 2M^{-1}\langle(\tilde{f}_{\mathrm{a}}/\tilde{f}_0)^2\rangle + \mathrm{o}(M^{-1}).\end{aligned}$$

Recall, that $\chi_M^2(1-\alpha) = \frac{1}{2}(\Phi^{-1}(1-\alpha)+\sqrt{2M-1})^2 + \mathrm{o}(1)$, where $\Phi(\cdot)$ represents the cumulative distribution function of a standard normal random variable. Hence, we have that

$$\begin{aligned}P(\alpha;\boldsymbol{\mu},\mathbf{C}) = \Pr\{z_M \geq \frac{M^{-1}\chi_M^2(1-\alpha) - \tilde{\mu}_{Q,M}}{\tilde{\sigma}_{Q,M}}\}\\ \approx 1 - \Phi[\sqrt{M}(\frac{1-\langle\tilde{f}_{\mathrm{a}}/\tilde{f}_0\rangle}{2\langle(\tilde{f}_{\mathrm{a}}/\tilde{f}_0)^2\rangle^{\frac{1}{2}}}) + \mathrm{o}(\sqrt{M})].\end{aligned}$$

Therefore, for a fixed significance level α, when $\langle\tilde{f}_{\mathrm{a}}/\tilde{f}_0\rangle > 1$ we have that $P(\alpha;\boldsymbol{\mu},\mathbf{C}) \to 1$ as $M \to +\infty$. Moreover, asymptotically the rate of convergence does not depend on the measurement noise intensity nor the time-reversed signal energy.

Unfortunately, in the case where $\langle \tilde{f}_{\rm a}/\tilde{f}_0 \rangle < 1$ the test does not behave well, for M large its power approaches zero. In particular, this shows that for a large M the MLR test is biased.

4.4.3. The modified MLR test In order to remedy this problem we slightly modify this test by introducing two-tailed rejection regions

$$\tilde{R}_\alpha = \{\mathbf{x} : Q_M(\mathbf{x}) \leq \chi^2_M(\alpha/2) \text{ or } Q_M(\mathbf{x}) \geq \chi^2_M(1-\alpha/2)\}.$$

Now, we have that the power of the modified test

$$\tilde{P}(\alpha; \boldsymbol{\mu}, \mathbf{C}) \approx 1 + \Phi(y_{l,M}\sqrt{M}) - \Phi(y_{r,M}\sqrt{M}),$$

where $y_{l,M} < y_{r,M}$ and

$$y_{\cdot,M} \to \frac{1 - \langle \tilde{f}_{\rm a}/\tilde{f}_0 \rangle}{2\langle (\tilde{f}_{\rm a}/\tilde{f}_0)^2 \rangle^{\frac{1}{2}}}$$

as $M \to +\infty$. Consequently, when $\langle \tilde{f}_{\rm a}/\tilde{f}_0 \rangle \neq 1$ we get that $\tilde{P}(\alpha; \boldsymbol{\mu}, \mathbf{C}) \to 1$. Again, asymptotically the convergence rate does not depend on the noise intensity nor the time-reversed signal energy.

Asymptotically, we are testing whether $\langle \tilde{f}_{\rm a}/\tilde{f}_0 \rangle$ is equal one or not. This quantity can be interpreted as an average (in frequency space) of the amplification/reduction ratio of the measurement-induced noise in the changed medium to the corresponding noise in the initial medium.

5. Numerical results

In order to establish how well the introduced detection technique works we carry out several Monte-Carlo simulations by numerically solving the model equations $(1a)$-$(1b)$. In doing that we address several key aspects of our approach to the detection problem. First, we illustrate the reliability of this detection technique by showing that the probability of detection observed in the simulations, is in complete agreement with the results predicted by the asymptotic theory, despite the fact that in simulations the small parameter ε is finite. Finally, we show the robustness of this technique to assumptions made in the asymptotic analysis.

5.1. Detecting an inclusion

In this series of simulations we address the realibility of the proposed detection technique. We illustrate how using time reversal enhances the signal to noise ratio when compared with relaying only on the reflected signals. Furthermore, we establish that the level of success of this detection test predicted from the asymptotic theory is actually achieved in the numerical simulations.

We consider the detection of an inclusion, that extends from $x = 25$ to $x = 50$, on an initial medium with a homogeneous background with $\varrho_{10} = K_{10} = 1$. The

relative changes induced by the inclusion in the background and local sound speed are approximately of 12.3% and 12.9%, respectively. We only consider random fluctuations of the media density which have a 30% maximum intensity and a 17% standard deviation. One realization of the profiles of the sound speed before and after inclusion is presented in figure 2. In the time reversal numerical procedure the incident pulse is a Gaussian of amplitude and width equal to one unit, and the recording time is $t_0 = 90$ time units. In the scaling we have chosen the small parameter $\varepsilon \approx 0.1$. The numerical solution of the corresponding acoustic equations is carried out using a Lagrangian numerical scheme with discretization stepsizes $\Delta t = \Delta x = 0.01$ (see details in [21]).

First, we carry out several time reversal experiments corresponding to an inclusion as depicted in figure 2 (upper left corner plot) for different levels of the measurement noise ($\sigma_\nu = 0.05 - 0.5$). In figure 1 we plot the signal to noise ratio associated to the reflected signals and the time-reversed difference reflection, respectively, with respect to the measurement noise intensity. It is apparent from the figure that time reversal enhances the signal to noise ratio, emphasizing the advantage of this approach.

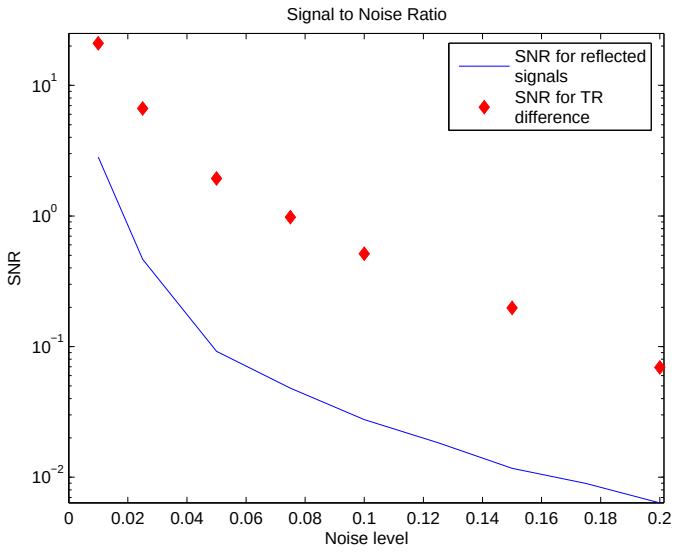

Figure 1. Signal to noise ratio corresponding to the reflected signals and the time-reversed difference reflection.

We made three sets of Monte-Carlo simulations corresponding to three different levels of the measurement noise ($\sigma_\nu = 0.05, 0.15$ and 0.50) with 500 realizations of the time reversal experiment per set.

In figure 2 we compare the ROCs corresponding to the asymptotic theory and the simulations. The theoretical ROCs are obtained from the appropriate expression of the power of the test $\tilde{P}(\cdot)$ by numerically evaluating the integral (43) after estimating the required parameters $\boldsymbol{\xi}$ and $\boldsymbol{\lambda}$ from the corresponding Monte-Carlo simulations. The ROC corresponding to simulations is obtained by computing the rate of success in each

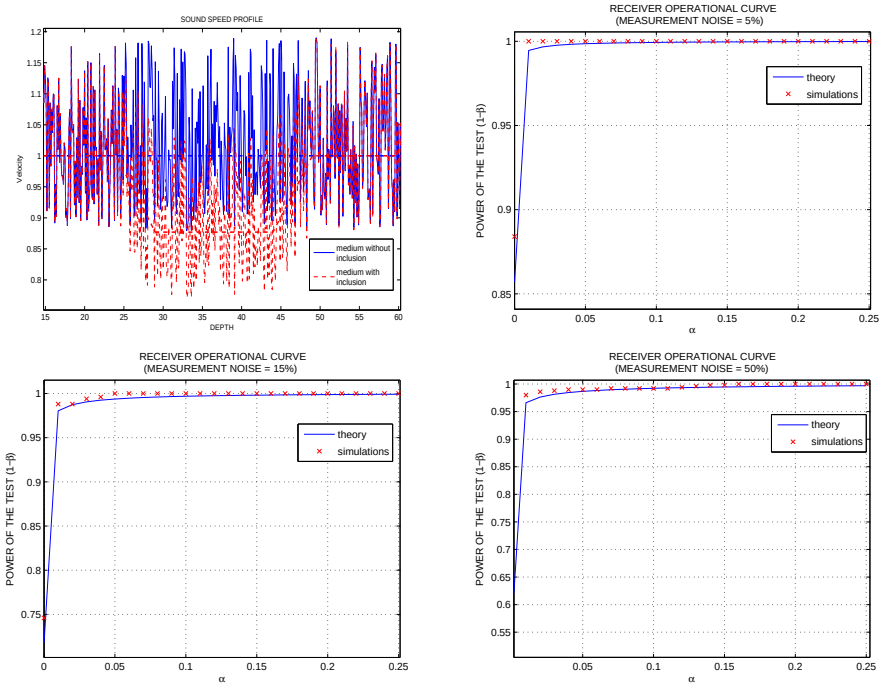

Figure 2. One realization of the profile of the propagation velocity corresponding to an inclusion. Theoretical Receiver Operating Curves (ROCs) and probability of detection obtained from a series of Monte-Carlo simulation with 500 realizations of the time reversal experiment using different values of the measurement noise ($\sigma_\nu = 0.05$, 0.15 and 0.50).

set of Monte-Carlo simulations for different levels of significance α. The test statistics is computed from samples with size $M = 200$ and time sampling rate $h = 0.01$. From this figure we conclude that there is a remarkable agreement between the ROCs from the asymptotic theory and the simulations. It is also apparent that the probability of detection is not very sensitive to the intensity of the measurement noise as predicted by our theory.

Finally, we briefly illustrate the influence of the time sampling rate h and the sample size M. In figure 3, the three ROCs corresponding to $(M, h) = (100, 0.02)$, $(100, 0.01)$ and $(200, 0.01)$, respectively, are shown. We can see that doubling the sample size produced a remarkable increase of the power of the test, whereas halving the sampling rate slightly reduced the power of the test.

5.2. Detecting a fluctuating slab

The next example concerns the robustness of the proposed detection technique. Recall that the corresponding statistical test was obtained under the assumption that the time-reversed difference reflection is statistically stable. However, this happens under very specific conditions, for instance when one has an increasing/decreasing velocity inclusion. Furthermore, in typical situations we do not know that these conditions

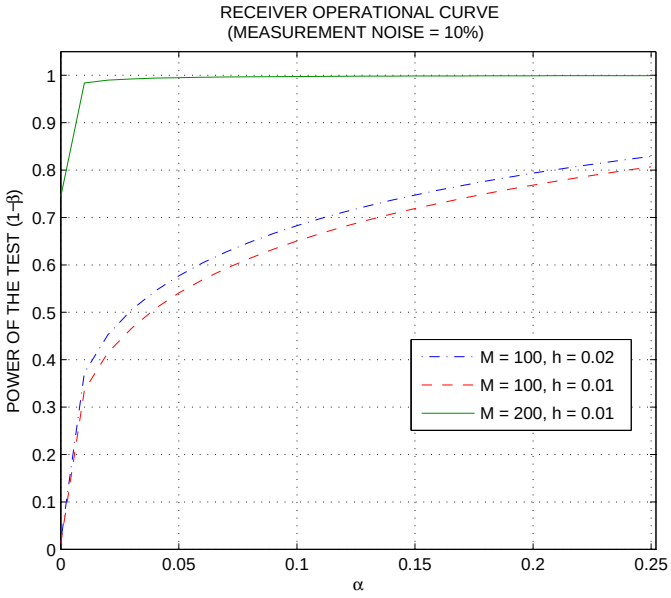

Figure 3. Comparison of the Theoretical Receiver Operating Curves (ROCs) for different sampling rates ($h = 0.01$ and 0.02) and different sample size ($M = 100$ and 200).

are fulfilled. Nonetheless, we show that the proposed detection technique is reliable under less restrictive conditions, namely in the case where the change occurs only in the fluctuations.

We let the fluctuations change only in the finite slab from $x = 24$ to $x = 44$ of the medium, while the background propagation velocity remains unchanged and equal to 1.

The first plot in figure 4 represents one realization of the profile of the sound speed. The time reversal setup is similar as in the previous section, we use the same incident Gaussian pulse, recording time $t_0 = 90$ and a small parameter $\varepsilon \approx 0.1$.

We run three sets of Monte-Carlo simulations corresponding to the measurement noise levels $\sigma_\nu = 0.05$, 0.15 and 0.50, with 500 realizations each, to estimate all the necessary parameters in order to apply the statistical test and obtain its probability of detection for different values of the level of significance α. The estimated parameters are also used to get the curves generated by $\tilde{P}(\cdot)$ using the equations corresponding to the statistically stable case.

The results are presented in figure 4. There is a remarkable agreement between the (statistically stable) power of the test curve and the probability of detection obtained in the Monte-Carlo simulations. The results are slightly better than those presented in the previous section, demonstrating that this approach may be very efficient for estimation in certain scaling regimes. Moreover, as in the previous section the results are not very sensitive to the intensity of the measurement noise.

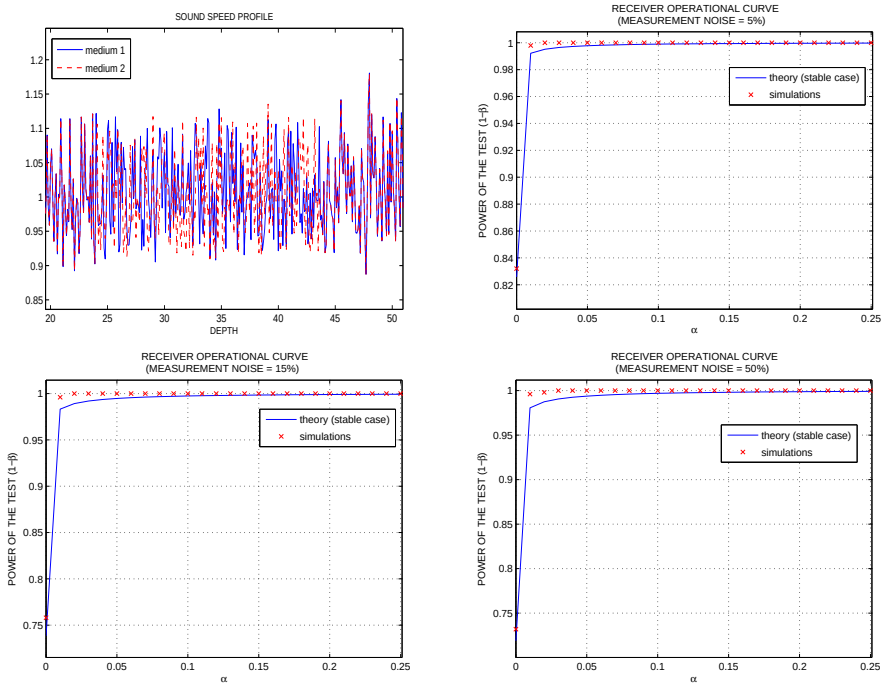

Figure 4. One realization of the profile of the propagation velocities corresponding to two media that only differ in terms of the fluctuations. Theoretical ROCs and probability of detection obtained from a series of Monte-Carlo simulation with 500 realizations of the time reversal experiment using different values of the measurement noise ($\sigma_\nu = 0.05$, 0.15 and 0.50).

6. Concluding remarks

In this paper, we introduce a statistical technique for the detection of inclusions in a random medium, that considers the effect of measurement errors. This detection technique relies on a time-reversal procedure and a statistical hypothesis testing approach. For the derivation of the statistical test, we take advantage of the asymptotic behaviour of the time-reversed difference signal as a small parameter ε, approaches zero.

The statistical test was specifically designed for the case where the time-reversed difference reflection satisfies the celebrated statistical stabilization property. We established this property for a situation that models a general class of inclusions.

Through a series of Monte-Carlo simulations we established the reliability of this detection technique when ε is small but finite, and we also established its robustness concerning the statistical stability property. More specifically, we showed that the probability of success of this detection test observed during simulations are in a remarkable agreement with those predicted by the asymptotic theory. Moreover, similar results are obtained in simulations where the statistical stability property is no longer valid. We also showed that by increasing the size of the sample we improve the performance of the detection technique.

Acknowledgments

This work was partially supported by DARPA grant N00014-02-1-0603, ONR grant N0014-02-1-0090, NSF grant 03070011 and the Sloan Foundation.

References

[1] Borcea, L., Papanicolaou, G. and Tsogka, C., 2005, Interferometric array imaging in clutter. *Inverse Problems*, **21**, 1419–1460.

[2] Borcea, L., Papanicolaou, G. and Tsogka, C., 2006, Coherent interferometry in finely layered random mediua. *SIAM J. Multiscale Model. Simul.*, **5**, 62–83.

[3] Borcea, L., Tsogka, C., Papanicolaou, G. and Berryman, J., 2002, Imaging and time reversal in random media. *Inverse Problems*, **18**, 1247–1279.

[4] Bal, G. and Pinaud, O., 2005, Time-reversal-based detection in random media. *Inverse Problems*, **21**(5), 1593–1619.

[5] Fouque, J.P. and Poliannikov, O., 2006, Time reversal detection in one-dimensional random media. *Inverse Problems*, **22**(3), 903–922.

[6] Poliannikov, O. and Fouque, J.P., 2005, Detection of a reflective layer in a random medium using time reversal. In: *Proceedings of the 2005 Int. Conf. on Acoustics, Speech and Signal Procesing*, March.

[7] Burridge, R., Papanicolaou, G., Sheng, P. and White, B., 1989, Probing a random medium with a pulse. *SIAM J. Appl. Math.*, **49**, 582–607.

[8] Asch, M., Kohler, W., Papanicolaou, G., Postel, M. and White, B., 1991, Frequency content of randomly scattered signals. *SIAM Review*, **33**, 519–626.

[9] Alfaro Vigo, D., 2004, Time-reversed acoustics in a randomly changing medium. PhD thesis, IMPA, Rio de Janeiro, Brazil.

[10] Alfaro Vigo, D., Fouque, J.P., Garnier, J. and Nachbin, A., 2004, Robustness of time reversal for waves in time-dependent random media. *Stoch. Processes Appl.*, **113**(2), 289–313.

[11] Krylov, N. and Rozovskii, B., 1982, Stochastic partial differential equations and diffusion processes. *Uspekhi Mat. Nauk*, **37**(6), 75–95 (transl. in Russian Math. Surveys, **37**:6(1982)).

[12] Kunita, H., 1990 *Stochastic flows and stochastic differential equations*, Cambridge Studies in Advanced Mathematics Vol. 24 (Cambridge: Cambridge University Press).

[13] Asch, M., Papanicolaou, G., Postel, M., Sheng, P. and White, B., 1990, Frequency content of randomly scattered signals. Part I. *Wave Motion*, **12**, 429–450.

[14] Papanicolaou, G., Postel, M., Sheng, P. and White, B., 1990, Frequency content of randomly scattered signals. Part II: Inversion. *Wave Motion*, **12**, 527–549.

[15] Rozanov, Y.A., 1967 *Stationary random processes* (Holden-Day) (translated from russian by A. Feinstein).

[16] Serfling, R., 1980 *Approximation theorems of mathematical statistics* (New York: John Wiley & Sons).

[17] Lehmann, E., 1986 *Testing statistical hypothesis*, second (New York: John Wiley & Sons).

[18] Johnson, N. and Kotz, S., 1970 *Distributions in statistics–Continuous Univariate Distributions*, Vol. 2 (New York: John Wiley & Sons).

[19] Ma, Y., Lim, T. and Pasupathy, S., 2002, Error probability for coherent and differential PSK over arbitrary Rician fading channels with multiple cochannel interferers. *IEEE Trans. Commun.*, **50**(3), 429–441.

[20] Grenander, U. and Szegö, G., 1958 *Toeplitz forms and their applications* (Berkeley: University of California Press).

[21] Alfaro Vigo, D., Correia, A.S. and Nachbin, A., 2007, Complete time-reversed refocusing in reflection with an acoustic Lagrangian model. *Commun. Math. Sci.*, **5**(1), 161–185.